Effects of Phosphorylation and Mutation R145G on Human Cardiac Troponin I Function †

ARTICLE *in* BIOCHEMISTRY · JANUARY 2002

Impact Factor: 3.02 · DOI: 10.1021/bi0115232 · Source: PubMed

6 AUTHORS, INCLUDING:

Kornelia Jaquet
Ruhr-Universität Bochum
47 PUBLICATIONS **1,172** CITATIONS
SEE PROFILE

Rolf Thieleczek
Ruhr-Universität Bochum
27 PUBLICATIONS **682** CITATIONS
SEE PROFILE

Effects of Phosphorylation and Mutation R145G on Human Cardiac Troponin I Function†

Yi Deng, Anja Schmidtmann, Alexander Redlich, Barbara Westerdorf, Kornelia Jaquet, and Rolf Thieleczek*

Institut für Physiologische Chemie, Abteilung für Biochemie Supramolekularer Systeme, Ruhr-Universität Bochum, D-44780 Bochum, Germany

Received July 20, 2001

ABSTRACT: We have studied functional consequences of the mutations R145G, S22A, and S23A of human cardiac troponin I (cTnI) and of phosphorylation of two adjacent N-terminal serine residues in the wild-type cTnI and the mutated proteins. The mutation R145G has been linked to the development of familial hypertrophic cardiomyopathy. Cardiac troponin was reconstituted from recombinant human subunits including either wild-type or mutant cTnI and was used for reconstitution of thin filaments with skeletal muscle actin and tropomyosin. The Ca^{2+}-dependent thin filament-activated myosin subfragment 1 ATPase (actoS1-ATPase) activity and the in vitro motility of these filaments driven by myosin were measured as a function of the cTnI phosphorylation state. Bisphosphorylation of wild-type cTnI decreases the Ca^{2+} sensitivity of the actoS1-ATPase activity and the in vitro thin filament motility by about 0.15−0.21 pCa unit. The nonconservative replacement R145G in cTnI enhances the Ca^{2+} sensitivity of the actoS1-ATPase activity by about 0.6 pCa unit independent of the phosphorylation state of cTnI. Furthermore, it mimics a strong suppressing effect on both the maximum actoS1-ATPase activity and the maximum in vitro filament sliding velocity which has been observed upon bisphosphorylation of wild-type cTnI. Bisphosphorylation of the mutant cTnI-R145G itself had no such suppressing effects anymore. Differential analysis of the effect of phosphorylation of each of the two serines, Ser23 in cTnI-S22A and Ser22 in cTnI-S23A, indicates that phosphorylation of Ser23 may already be sufficient for causing the reduction of maximum actoS1-ATPase activity and thin filament sliding velocity seen upon phosphorylation of both of these serines.

Troponin I is the inhibitory component of the troponin complex which is involved in the Ca^{2+}-dependent control of heart and skeletal muscle contraction. The heart specific isoform of TnI (cTnI)[1] contains two adjacent serine residues (positions 22 and 23 in the human cTnI sequence) in a N-terminal extension (*1*). cTnI forms a 1:1:1 complex with the cardiac specific isoforms of troponin C (cTnC) and troponin T (cTnT) which interacts with tropomyosin (Tm) and actin in the thin filament. The binding of Ca^{2+} to cTnC causes a cascade of conformational changes within the cardiac holotroponin complex (cTn) and consecutively in the thin filament which eventually allow force-generating interactions between actin and myosin (for review, see refs *2*−*4*). Heart muscle contraction is modulated by catecholamines which upon binding to adrenoceptors lead to phosphorylation of several proteins involved in the contractile process (*5*−*10*). cTnI is phosphorylated upon β_1-adrenergic stimulation by the cAMP-dependent protein kinase (PKA) at the two cardiac specific residues, Ser22 and Ser23 (*1*), and phosphorylation of these serines reduces the apparent Ca^{2+} affinity of cTnC (*11, 12*) as well as the Ca^{2+} sensitivity of force production (*13*). These events have been correlated with an enhanced relaxation rate of the contractile system (*14*). A reduced degree of cTnI phosphorylation has been observed in failing hearts which would be in agreement with an increased Ca^{2+} sensitivity of the contractile apparatus in these tissues (*15*, *16*).

Recently, several mutations in the gene of human cTnI have been linked to the development of familial hypertrophic cardiomyopathy (fHCM) (*17*, *18*). These mutations are located in the inhibitory region of cTnI and further downstream in the C-terminal part. Both regions are involved in

† Supported by the Deutsche Forschungsgemeinschaft (SFB 394), FORUM F190/00 of the Medical Faculty of the Ruhr-Universität Bochum, and the Hans and Gertie Fischer Stiftung.

* To whom correspondence should be addressed. Phone: (+49) (0)-234 32 25291. Fax: (+49) (0)234 32 14193. E-mail: rolf.thieleczek@ruhr-uni-bochum.de.

[1] Abbreviations: actoS1-ATPase, thin filament-activated myosin S1-ATPase; cTn, cardiac troponin; cTnI, cTnC, and cTnT, cardiac troponin I, C, and T, respectively; cTnI-WT/dd and cTnI-WT/pp, nonphosphorylated and bisphosphorylated wild-type cTnI, respectively; cTnI-R145G, R145G-mutated cTnI; cTnI-R145G/dd and cTnI-R145G/pp, nonphosphorylated and bisphosphorylated cTnI-R145G, respectively; cTnI-S22A/d and cTnI-S22A/p, nonphosphorylated and monophosphorylated S22A-mutated cTnI, respectively; cTnI-S23A/d and cTnI-S23A/p, nonphosphorylated and monophosphorylated S23A-mutated cTnI, respectively; DTT, dithiothreitol; EGTA, ethylene glycol bis(β-aminoethyl ether)-*N*,*N*,*N*′,*N*′-tetraacetic acid; EDTA, ethylenediaminetetraacetic acid; F-actin, actin filaments; fHCM, familial hypertrophic cardiomyopathy; HEPES, *N*-(2-hydroxyethyl)piperazine-*N*′-2-ethanesulfonic acid; HPLC, high-performance liquid chromatography; MESG, 2-amino-6-mercapto-7-methylpurine riboside; MOPS, 3-(*N*-morpholino)propanesulfonic acid; PAGE, polyacrylamide gel electrophoresis; PKA, cAMP-dependent protein kinase; PMSF, phenylmethylsulfonyl fluoride; PNP, purine nucleoside phosphorylase; SDS, sodium dodecyl sulfate; S1, myosin subfragment 1; Tm, tropomyosin; TRITC, tetramethylrhodamine 5- (and 6-) isothiocyanate. Amino acids are given in either the one- or the three-letter code.

10.1021/bi0115232 CCC: $20.00
Published on Web 11/07/2001

Ca^{2+}-dependent interactions of cTnI with other proteins of the thin filament. It has been proposed that some of these mutations in cTnI (R145G, R162W) may affect relaxation rather than contraction of cardiac muscle (*18*).

However, so far studies on the functional consequences of cTnI mutant proteins linked to fHCM did not consider the cTnI phosphorylation state which, according to the results mentioned before, is an important parameter in determining cardiac performance. Therefore, we have investigated in vitro functions of R145G mutant cTnI (cTnI-R145G) in the nonphosphorylated (cTnI-R145G/dd) and bisphosphorylated (cTnI-R145G/pp) states and those of the S22A and S23A mutants of cTnI in the nonphosphorylated (cTnI-S22A/d and cTnI-S23A/d, respectively) and monophosphorylated states (cTnI-S22A/p and cTnI-S23A/p, respectively). They were compared with those of the nonphospho (cTnI-WT/dd) and bisphospho forms (cTnI-WT/pp) of wild-type cTnI. Thin filaments were reconstituted from these human cTnI species and human cTnC and cTnT, all obtained by recombinant techniques, and actin and Tm purified from skeletal muscle. The functional properties of these eight types of reconstituted thin filaments were investigated by measuring the thin filament-activated myosin subfragment 1 (S1) ATPase activity (actoS1-ATPase activity) and the in vitro motility of the thin filaments propelled by surface-bound myosin as a function of the free Ca^{2+} concentration.

This approach allows the comparison of enzymatic and mechanoenzymatic properties of regulated actomyosin complexes under comparable experimental conditions. It reveals a new suppressing effect of phosphorylation of both serines, Ser22 and Ser23, as well as of mutation R145G of cTnI on the maximum actoS1-ATPase activity and the maximum in vitro sliding velocity. It also indicates that phosphorylation of Ser23 may already be sufficient for causing these effects.

EXPERIMENTAL PROCEDURES

Expression of Human cTnT. The cDNA of human cTnT obtained as clone HCTNNT2 (*19*) was amplified by polymerase chain reaction with the following primers: 5′-GAA TTC ATA TGT CTG ACA TAG AAG AGG TGG-3′ and 5′-AAG CTT GGA TCC CTA TTT CCA GCG CCC GGT GAC-3′. A *Nde*I and a *Bam*HI recognition site was introduced for subcloning into the *Nde*I−*Bam*HI site of the pSBETc vector (*20*). Human cTnT was expressed in *Escherichia coli* BL21(DE3). The cells were grown in NZCYM medium (Difco) with 0.3 mg/mL kanamycin at 37 °C until an $OD_{600} = 0.6$ was reached. cTnT expression was induced by addition of isopropyl 1-thio-β-D-galactopyranoside to a final concentration of 0.4 mM. The cells were harvested after a further incubation for 4 h.

DNA Sequencing. The cDNA sequences coding for wild-type or mutant proteins were checked by automatic sequencing of both strands (ABIPRISM 377 DNA sequencer, Perkin-Elmer) using the ABIPRISM big dye deoxy terminator cycle sequencing ready reaction kit.

Purification of Recombinant Human cTnT. Cell pellets from a 2 L culture were resuspended in 20 mL of 25 mM Tris-HCl, pH 7.5, 20% sucrose, 1 mM EDTA, 0.3 mM PMSF, 0.2 M NaCl, 5 μg/mL *N*-tosyl-L-phenylalanine chloromethyl ketone, and 5 μg/mL N^{α}-*p*-tosyl-L-lysine chloromethyl ketone and frozen overnight at −80 °C. After thawing, the cells were fractured by French press treatment and then 5 M ultrapure urea and Triton X-100 (0.1% v/v) were added. The suspension was stirred for 1 h at 4 °C and then centrifuged at 120000*g* for 1 h at 4 °C. The supernatant was diluted 1:10 with equilibration buffer containing 50 mM Tris-HCl, pH 7.5, 5 mM $CaCl_2$, 1 mM $MgCl_2$, 1 mM DTT, and 5 M urea. The solution was combined with 100 mL of anion exchanger DE52 (Whatman) equilibrated in equilibration buffer. After incubation for 2 h at 4 °C the suspension was filled into a column (diameter: 2.5 cm), and cTnT was eluted at a flow rate of 0.5 mL/min with a linear gradient of 0.1−0.5 M NaCl in equilibration buffer and collected in 4 mL fractions. The cTnT-containing fractions were combined and applied on a gel filtration column (Pharmacia G-75 superfine, 2.5 × 60 cm) equilibrated with 50 mM Tris-HCl, pH 7.5, 0.5 M NaCl, 5 mM $CaCl_2$, 1 mM $MgCl_2$, and 2 mM DTT. cTnT was eluted at a flow rate of 12 mL/h and collected in 3 mL fractions. Purified protein (about 10 mg of cTnT/L of culture) was stored at −20 °C.

Expression and Purification of Human cTnC. Human cTnC was overexpressed in *E. coli* (*21*) and purified using anion-exchange (DE52, Whatman) and affinity chromatography (phenyl-Sepharose CL-4B, Pharmacia) (*22*). About 100 mg of cTnC/L of culture was obtained.

Expression and Purification of Wild-Type Human Cardiac TnI, cTnI-S22A, and cTnI-S23A. Wild-type human cTnI and the cTnI mutants S22A and S23A were obtained as described previously (*21*). Briefly, *E. coli* BL21 (DE3) was transformed by a pET3c vector containing the corresponding cDNA of cTnI. The proteins were overexpressed and purified using CM-Sepharose fast flow (Pharmacia) and cTnC affinity material (*21*). The final yield of each cTnI species was approximately 20 mg/L of culture.

Site-Directed Mutagenesis and Expression of Human cTnI-R145G. To create the cTnI-R145G mutant, the following oligonucleotides were used: 5′-CGG CCC ACC CTG GGG AGA GTG AGG-3′ and 5′-CCT CAC TCT CCC CAG GGT GGG CCG-3′. The mutation at codon 145 from CGG (Arg) to GGG (Gly) was generated using the QuickChange site-directed mutagenesis kit (Stratagene). Wild-type as well as R145G mutant protein was expressed in *E. coli* BL21 (DE3). The cells were grown in NZCYM medium with 0.2 mg/mL ampicillin at 37 °C until an $OD_{600} = 0.6$ was reached. cTnI expression was induced with 0.4 mM β-thiogalactopyranoside, and the cells were harvested after a further 4 h incubation at 37 °C. Expression was controlled using SDS−PAGE. The protein bands were analyzed by scanning densitometry using the Whole Band Analyzer Software (Bioimage, U.K.). cTnI, which makes up about 13% of the total protein was identified by immunoblotting.

Purification and Characterization of Human cTnI-R145G. R145G mutant cTnI was isolated as described for wild-type cTnI (*21*). Additionally, a final gel filtration step was carried out on Sephadex G-75 superfine (Pharmacia, column diameter 2.5 cm, volume 400 mL). The protein was eluted at a flow rate of 15 mL/h with 50 mM Tris-HCl, pH 7.5, 0.5 M NaCl, and 2 mM DTT. The final yield was about 5−10 mg of cTnI-R145G/L of culture which was stable against proteolysis for at least 25 days at 4 °C. The mass of human cTnI-R145G of 23777 Da determined by electrospray ionization mass spectrometry (*23*) was identical to the calculated mass.

Reconstitution of Human cTn. Human cTn was reconstituted by mixing cTnT, cTnC, and either wild-type or mutant cTnI (S22A, S23A, or R145G) at a molar ratio of 1:1:1 (13 μM each) in urea buffer (50 mM Tris-HCl, pH 8.0, 6 M urea, 0.5 M NaCl, 5 mM $CaCl_2$, 7 mM DTT). The mixture was gently shaken for 2 h at room temperature and then stepwise dialyzed against a high salt buffer (1 M KCl, 10 mM MOPS/KOH, pH 7.0, 1.25 mM $MgCl_2$, 1.25 mM $CaCl_2$, 1.5 mM DTT) containing decreasing urea concentrations (4, 2, and 0 M). Thereafter, the salt content of the protein solution was also reduced step by step introducing subsequently 1, 0.7, 0.5, and 0.3 M KCl in the same buffer as before. Reconstitution of the cTn complex was checked by gel filtration (Pharmacia Sephadex G-75 superfine, column diameter 0.9 cm, volume 80 mL, flow rate 5 mL/h) and monitoring the protein content of the eluate by protein determination (*24*), the protein purity by SDS−PAGE [15% homogeneous polyacrylamide (*25*)], and the 1:1:1 complex formation by gel scanning using Whole Band Analyzer Software (Bioimage, U.K.) and a bovine cTn as standard. If necessary, uncomplexed subunits were separated from the cTn complex by gel filtration on Sephadex G-75 on a preparative scale.

Phosphorylation of Human cTnI in the cTn Complex. Fractions containing holo-cTn were combined and used for phosphorylation of the actual cTnI in the complex. Wild-type cTnI and cTnI-R145G were phosphorylated at both serine residues, 22 and 23, and cTnI-S22A and cTnI-S23A at the serine still present in the mutant cTnI. cTn was dialyzed overnight against 20 mM MOPS/KOH, pH 7.0, 0.3 M KCl, and 1 mM DTT. Phosphorylation was initiated by addition of 5 mM $MgCl_2$, 1 mM ATP, and a catalytic subunit of PKA (160 milliunits/mg cTnI-WT, 120 milliunits/mg cTnI-R145G, 45 milliunits/mg cTnI-S22A, 90 milliunits/mg cTnI-S23A) to this buffer. The reaction was carried out at 30 °C and stopped after 90 min by drop freezing in liquid nitrogen which irreversibly inactivates PKA. The phosphorylation state of cTnI was checked by isoelectric focusing (*23*) following separation of cTnI from the cTn complex by reversed-phase HPLC (*26*). Only cTn containing either bisphosphorylated wild-type cTnI and cTnI-R145G, respectively, or monophosphorylated cTnI-S22A and cTnI-S23A, respectively, was used for filament reconstitution.

Thin Filament Reconstitution. Actin (*27*) and Tm (*28*) were isolated from rabbit skeletal muscle. Actin was polymerized in 100 mM KCl, 1 mM $MgCl_2$, 5 mM triethanolamine-HCl, pH 7.5. Purified Tm and the reconstituted human cTn were dialyzed overnight at 4 °C against 150 mM KCl, 20 mM HEPES/KOH, pH 7.5, and 2 mM DTT. Thin filaments were reconstituted in reconstitution buffer (20 mM HEPES/KOH, pH 7.5, 70 mM KCl, 5 mM $MgCl_2$, 0.5 mM EGTA, 2 mM DTT) from polymerized actin (8 μM), Tm (2 μM), and reconstituted cTn (2 μM) containing either wild-type or mutant cTnI in defined phosphorylation states (see above). The protein solution was incubated overnight at 4 °C. To obtain thin filaments containing nonphosphorylated wild-type or mutant cTnI, these filaments were dephosphorylated with protein phosphatase 2A as described previously (*12*). Reconstituted thin filaments containing either cTnI-WT/dd, cTnI-WT/pp, cTnI-S22A/d, cTnI-S22A/p, cTnI-S23A/d, cTnI-S23A/p, cTnI-R145G/dd, or cTnI-R145G/pp were dialyzed overnight against reconstitution buffer.

ActoS1-ATPase Assay. Myosin was isolated from rabbit back muscle (*29*), and myosin S1 was obtained by papain digestion (*29*). Myosin S1-ATPase activity and actoS1-ATPase activity activated by each of the eight types of reconstituted thin filaments (see above) at various free Ca^{2+} concentrations were measured according to a modified method (*30*) in a sample volume of 200 μL. ATPase activity measurements in the presence of naked F-actin instead of reconstituted thin filaments under the same experimental conditions served as controls. Reconstituted thin filaments were added to assay buffer establishing finally 0.2 mM MESG (Molecular Probes), 12.5 units/mL PNP (Sigma-Aldrich), 20 mM HEPES/KOH, pH 7.5, 5 mM DTT, 2 mM ATP, 35 mM KCl, 5.25 mM EGTA, 2 mM free Mg^{2+}, various free Ca^{2+} concentrations in the range of 0.1 nM to 10 μM, and 4 μM F-actin assembled with Tm and cTn at a molar ratio of 4:1:1 (see Thin Filament Reconstitution). The free Ca^{2+} concentrations were adjusted by mixing balanced CaEGTA- and EGTA-containing solutions (*31*). The total concentrations of Mg^{2+} and Ca^{2+} needed were calculated using affinity constants for EGTA and ATP derived from compiled values (*32*). An aliquot of this assay solution was transferred to a microcuvette, and the reaction was started by addition of 0.5 μM myosin S1. The absorbance change at 360 nm was monitored for 1−2 min at room temperature using a UVIKON933 spectrophotometer (Kontron Instruments). The assay was calibrated using phosphate standard solutions in the range of 2−25 μM.

In Vitro Motility Assay. The eight types of reconstituted thin filaments (see above) were labeled fluorescently with phalloidin−TRITC (*33*). Unregulated F-actin which was labeled in the same way was employed as control. The in vitro motility assay was carried out according to ref *33*, employing 0.2−0.4 mg/mL myosin and 1.2−3.6 nM reconstituted thin filaments containing either cTnI-WT/dd, cTnI-WT/pp, cTnI-S22A/d, cTnI-S22A/p, cTnI-S23A/d, cTnI-S23A/p, cTnI-R145G/dd, or cTnI-R145G/pp. ATP-insensitive myosin molecules were excluded from usage by actin affinity purification (*33*). The experimental conditions of the motility assay were similar to those of the ATPase assay (25 mM imidazole-HCL, pH 7.5, 5 mM EGTA, 2 mM ATP, 2 mM free Mg^{2+}, 35 mM KCl, and various free Ca^{2+} concentrations in the range given above). A scavenging system (*33*) consisting of 20 mM DTT, 0.5 mg/mL BSA, 3 mg/mL glucose, 0.1 mg/mL glucose oxidase, and 20 μg/mL catalase was used. The assay was carried out at room temperature under a fluorescence microscope (Nikon E400, 60 × 1.4 NA objective, filter block G-1B, 100 W Hg arc lamp) equipped with a CCD-video camera (MS-168EP, The Imaging Source) for recording the sliding movement of the reconstituted thin filaments on videotape. Recording was done for 15−30 s each at 7−12 different places of a flow cell. The recordings were digitized by means of a standard frame grabber card connected to a computer using a capturing rate of 1−2 frames/s. Filament paths were tracked and analyzed using the software RETRAC (*35*) and evaluated according to "smooth moving" criteria (*36*).

Data Analysis. The data obtained from actoS1-ATPase activity and thin filament mean sliding velocity measurements were normalized to the corresponding data obtained with naked F-actin under the same experimental conditions. Data sets were analyzed to give mean ± SEM. Mean sliding

velocities and standard deviations obtained from single filaments at a given pCa were combined to get the weighted mean ± SEM of all filaments at this pCa. The fraction of moving filaments at each pCa was determined from the number of moving filaments and the total number of filaments in a randomly selected area of the flow cell. Both, the Ca^{2+}-dependent normalized ATPase activity and the mean sliding velocity were fit to the Hill equation

$$y(\mathrm{pCa}) = a + b/(1 + 10^{n(\mathrm{pCa}-\mathrm{pCa}_{50})}) \quad (1)$$

to obtain parameter estimates and standard errors for the absolute signal at pCa ≫ pCa_{50}, *a*, the amplitude of the Ca^{2+}-dependent response, *b*, the Hill coefficient, *n*, and the midpoint pCa value, pCa_{50}. The parameters describing the Ca^{2+}-dependent activation processes themselves were obtained by normalizing the difference between mean values to the maximum difference of the mean values of a data set. These relative data were fit to the function

$$Y(\mathrm{pCa}) = 1/(1 + 10^{\mathrm{nH}(\mathrm{pCa}-\mathrm{pCa}_{\mathrm{H}})}) \quad (2)$$

to obtain the midpoint pCa, pCa_H, and the steepness, nH, of these sigmoidal curves. Statistical analysis of the data was performed using Student's *t*-test. Values were defined as significantly different with *p* values <0.05.

RESULTS

The method established for measuring thin filament-activated myosin S1-ATPase activity using MESG/PNP is exemplified in Figure 1 with nonphosphorylated wild-type cTnI. The absorbance coefficient of MESG ($\epsilon = 1.12 \times 10^4$ M^{-1} cm^{-1}) determined under the experimental conditions employed is in agreement with data reported previously (*30*, *36*) and is shown here to be independent of Ca^{2+}. Thus, Ca^{2+}-dependent changes in actoS1-ATPase activity, corrected by the ATPase activity of myosin S1 alone, are reflecting Ca^{2+}-mediated alterations in the actomyosin interaction. The actoS1-ATPase activity normalized to the activity of myosin S1-ATPase activated by naked F-actin under the corresponding experimental conditions shows a sigmoidal rise with increasing free Ca^{2+} concentrations for wild-type and R145G mutant cTnI in both the non- and the bisphosphorylated states (Figure 2). The maximum actoS1-ATPase activity obtained with nonphosphorylated wild-type cTnI is about 24% higher than that obtained in the presence of naked F-actin (later also termed reference level; Figure 2A). Bisphosphorylation of wild-type cTnI significantly ($p < 0.001$) reduces this maximum ATPase activity to about 75% of the reference level. The parameters of the fit curves which describe these and further results are compiled in Table 1. The maximum actoS1-ATPase activity obtained with R145G mutant cTnI in either phosphorylation state (Figure 2B) is similar to the maximum activity level obtained with cTnI-WT/pp (Figure 2A). These activity levels in the presence of cTnI-R145G/dd, cTnI-R145G/pp, and cTnI-WT/pp (43%, 53%, and 75% of the reference level, respectively; Table 1) are statistically not significantly different. In contrast, the maximum actoS1-ATPase obtained with cTnI-R145G/dd is significantly lower ($p < 0.005$) than that of cTnI-WT/dd (43% and 124% of the reference level; Table 1). The basal actoS1-ATPase activity levels measured at pCa 9.8 with all four types of

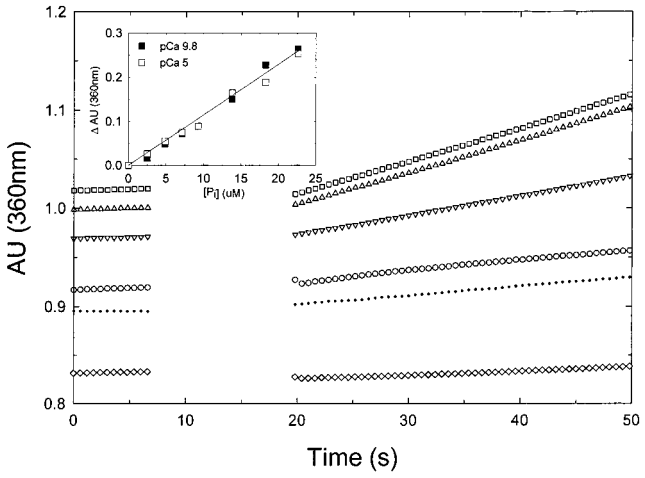

FIGURE 1: Monitoring of actoS1-ATPase activity controlled by reconstituted thin filaments. ATP hydrolysis by the filament-activated myosin S1-ATPase was measured spectrophotometrically at 360 nm with different free Ca^{2+} concentrations (pCa 9.8, ○; pCa 6.5, ●; pCa 6, ▽; pCa 5.5, □; pCa 5.0, △) using MESG/PNP (*28*). The assays were carried out under standard conditions in the presence of 4 μM F-actin, 1 μM Tm, and 1 μM cTn containing cTnI/dd-WT in this example (see Experimental Procedures). The reaction was started with 0.5 μM myosin S1 added during the time period represented by the gap. The rate of ATP hydrolysis was obtained by applying a common absorbance coefficient of 1.12×10^4 M^{-1} cm^{-1} derived from P_i standard curves as shown in the inset (pCa 9.8, 0.0115 ± 0.0004 AU/μM; pCa 5, 0.0108 ± 0.0002 AU/μM). The ATPase activities measured in the given pCa range 9.8−5.0 are 17.9, 17.6, 37.6, 63.3, and 63.1 pmol/s, respectively. ◇ depicts the Ca^{2+}-independent change in P_i concentration solely due to myosin S1-ATPase (no thin filaments present) at 8.9 pmol/s. The background formation of P_i in the absence of myosin S1 (initial phases before the gap) is negligible (<0.4 pmol/s).

reconstituted thin filaments independent of mutation or phosphorylation state of cTnI (8−23% of the reference level; Table 1) are not significantly different. The Ca^{2+}-dependent activation process of actoS1-ATPase leading from the basal to the maximum activity level is shown in Figure 2C,D. A significant decrease in the Ca^{2+} sensitivity is observed due to bisphosphorylation of wild-type cTnI ($\Delta pCa_{50} = 0.21 \pm 0.06$, $p < 0.005$; Figure 2C). The apparent shift in pCa_{50} due to bisphosphorylation of R145G mutant cTnI (Figure 2D) is, however, statistically not significant. ActoS1-ATPase activities controlled by R145G mutant cTnI were significantly more sensitive ($p < 0.0001$) toward Ca^{2+} than those controlled by wild-type cTnI (compare panels C and D of Figure 2; $\Delta pCa_{50} = 0.58 \pm 0.07$ for cTnI-WT/dd and cTnI-R145G/dd; $\Delta pCa_{50} = 0.63 \pm 0.12$ for cTnI-WT/pp and cTnI-R145G/pp). Neither the mutation R145G nor the bisphosphorylation of cTnI significantly influenced the cooperativity of the Ca^{2+}-dependent activation process of actoS1-ATPase.

The reconstituted thin filaments used in the ATPase activity assay above were subjected also to an in vitro motility assay under similar experimental conditions in order to study the mechanical output resulting from the molecular interactions leading to activation of actoS1-ATPase. The average mean sliding velocity of reconstituted thin filaments propelled by myosin at a given pCa (Figure 3) was obtained from combined velocity profiles of single filaments measured under these conditions. The average mean sliding velocity of reconstituted thin filaments normalized to that of phalloidin−TRITC-stabilized F-actin under the corresponding experimental conditions (Figure 3A,B) shows the same

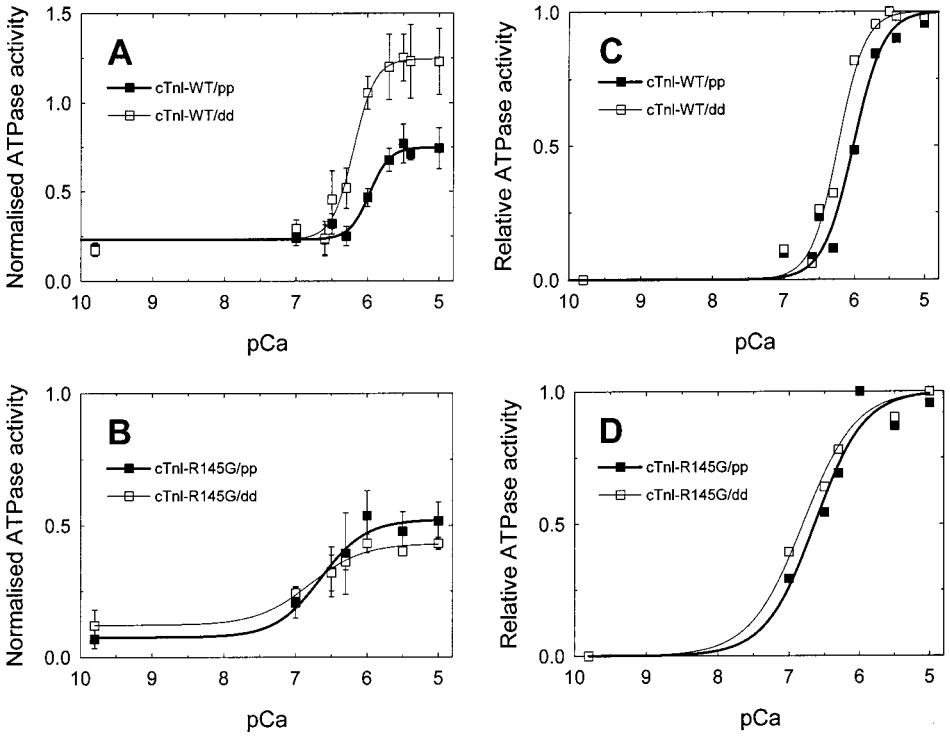

FIGURE 2: Ca^{2+}-dependent regulation of actoS1-ATPase by thin filaments containing wild-type (A, C) or R145G mutant (B, D) cTnI in either the non- or the bisphosphorylated state. (A, B) Thin filament-activated myosin S1-ATPase activity (mean values ± SEM) normalized to the F-actin-activated myosin S1-ATPase activity measured under the corresponding conditions (50.6 ± 7.1 pmol/s). The curves represent nonlinear least-squares fits to the data employing eq 1 (see Experimental Procedures). The values of the fit parameters *a*, *b*, pCa_{50}, and *n* are compiled in Table 1. (C, D) Rise in actoS1-ATPase activity normalized to the maximum difference of the corresponding data in (A) and (B). The curves represent nonlinear least-squares fits to the data employing eq 2 (see Experimental Procedures). The values of the fit parameters pCa_H and nH are 6.22 ± 0.03, 2.47 ± 0.35 (cTnI-WT/dd); 6.01 ± 0.05, 2.02 ± 0.33 (cTnI-WT/pp); 6.80 ± 0.07, 1.16 ± 0.21 (cTnI-R145G/dd); and 6.64 ± 0.08, 1.25 ± 0.28 (cTnI-R145G/pp).

Table 1: Summary of Parameters Describing the Ca^{2+}-Dependent Activation of ActoS1-ATPase Activity and Thin Filament in Vitro Motility[a]

	actoS1-ATPase activity[b]							
	cTnI-WT/dd	cTnI-WT/pp	cTnI-R145G/dd	cTnI-R145G/pp	cTnI-S22A/d	cTnI-S22A/p	cTnI-S23A/d	cTnI-S23A/p
a	0.23 ± 0.04	0.23 ± 0.02	0.12 ± 0.03	0.08 ± 0.05	0.07 ± 0.09	0.22 ± 0.05	0.07 ± 0.06	0.16 ± 0.03
b	1.01 ± 0.06	0.52 ± 0.04	0.31 ± 0.03	0.45 ± 0.06	1.00 ± 0.14	0.67 ± 0.09	0.64 ± 0.11	0.44 ± 0.06
c[d]	1.24 ± 0.08	0.75 ± 0.08	0.43 ± 0.14	0.53 ± 0.21	1.07 ± 0.21	0.89 ± 0.16	0.71 ± 0.24	0.60 ± 0.15
pCa_{50}	6.20 ± 0.04	5.97 ± 0.05	6.80 ± 0.12	6.65 ± 0.14	6.00 ± 0.09	5.80 ± 0.10	5.95 ± 0.13	5.93 ± 0.09
n	2.89 ± 0.61	3.09 ± 1.09	1.17 ± 0.37	1.38 ± 0.53	2.34 ± 0.97	2.48 ± 1.12	1.80 ± 0.84	2.60 ± 1.23
N	11	14	3	3	5	5	3	5
	mean filament sliding velocity[c]							
	cTnI-WT/dd	cTnI-WT/pp	cTnI-R145G/dd	cTnI-R145G/pp	cTnI-S22A/d	cTnI-S22A/p	cTnI-S23A/d	cTnI-S23A/p
a	0.24 ± 0.04	0.34 ± 0.05	0.40 ± 0.07	0.38 ± 0.08	0.06 ± 0.04	0.14 ± 0.06	0.04 ± 0.05	0.14 ± 0.04
b	0.89 ± 0.05	0.46 ± 0.07	0.56 ± 0.12	0.50 ± 0.15	0.86 ± 0.06	0.65 ± 0.08	0.84 ± 0.06	0.61 ± 0.05
c[d]	1.13 ± 0.08	0.80 ± 0.15	0.96 ± 0.20	0.88 ± 0.26	0.92 ± 0.11	0.79 ± 0.18	0.88 ± 0.13	0.75 ± 0.12
pCa_{50}	6.39 ± 0.04	6.27 ± 0.11	6.40 ± 0.22	6.28 ± 0.28	6.47 ± 0.05	6.59 ± 0.13	6.42 ± 0.05	6.54 ± 0.08
n	2.29 ± 0.51	2.29 ± 1.24	1.02 ± 0.53	1.10 ± 0.77	1.57 ± 0.42	1.53 ± 0.90	1.93 ± 0.50	1.72 ± 0.69
N	5	5	3	3	4	4	4	4

[a] The basal level at pCa 9.8, *a*, the amplitude of the Ca^{2+}-dependent rise, *b*, the midpoint pCa, pCa_{50}, and the Hill coefficient, *n*, were determined by fitting eq 1 to the data. The parameters are expressed as mean values ± SEM of *N* experiments. [b] Normalized to the actoS1-ATPase activity in the presence of F-actin. [c] Normalized to the mean sliding velocity of F-actin. [d] $c = a + b$ is the maximum level of actoS1-ATPase activity and the mean filament sliding velocity, respectively.

general behavior as the actoS1-ATPase activated by these filaments. The maximum velocity obtained with nonphosphorylated wild-type cTnI is about 13% higher than that observed in the presence of unregulated F-actin (later also termed reference velocity; Figure 3A and Table 1). In analogy to the actoS1-ATPase activity, bisphosphorylation of wild-type cTnI reduces this maximum velocity to about 80% of the reference velocity, which is significantly lower ($p < 0.05$) than that controlled by cTnI-WT/dd (Table 1). Likewise, the maximum normalized mean sliding velocities obtained with R145G-mutated cTnI in the non- and the bisphosphorylated state (Figure 3B, 96% and 88% of reference velocity) and with cTnI-WT/pp (Figure 3A, 80% of reference velocity) are not significantly different (Table 1). But there is an apparent difference between the maximum velocity of thin filaments reconstituted with cTnI-WT/dd and cTnI-R145G/dd (Figure 3A,B). However, this turned out not to be significant when estimating the maximum velocity at

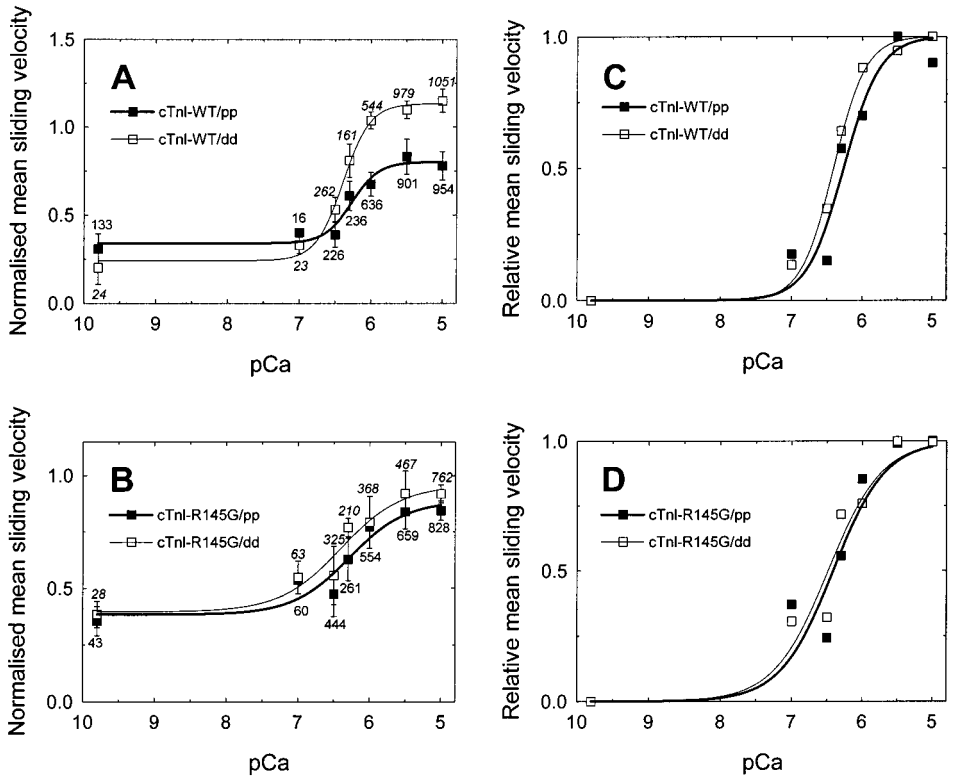

FIGURE 3: Ca^{2+}-dependent mean sliding velocity of regulated thin filaments containing wild-type (A, C) or R145G mutant (B, D) cTnI in either the non- or the bisphosphorylated state. (A, B) Mean sliding velocity (mean values ± SEM) normalized to the mean sliding velocity of naked phalloidin−TRITC-stabilized F-actin measured under the corresponding conditions (1.64 ± 0.02 μm/s). The number of filament paths of a data set is given by the number close to the corresponding error bar (italic for nonphosphorylated cTnI). The curves represent nonlinear least-squares fits to the data employing eq 1 (see Experimental Procedures). The values of the fit parameters *a*, *b*, pCa_{50}, and *n* are compiled in Table 1. (C, D) Increase in mean sliding velocity normalized to the maximum difference of the corresponding data in (A) and (B). The curves represent nonlinear least-squares fits to the data employing eq 2 (see Experimental Procedures). The values of the fit parameters pCa_H and nH are 6.41 ± 0.03, 1.90 ± 0.26 (cTnI-WT/dd); 6.26 ± 0.07, 1.68 ± 0.52 (cTnI-WT/pp); 6.48 ± 0.10, 1.14 ± 0.32 (cTnI-R145G/dd); and 6.41 ± 0.12, 1.17 ± 0.44 (cTnI-R145G/pp).

saturating free Ca^{2+} concentrations, *c*, from the determined fit parameters *a* and *b* (Table 1). This estimate is prone to error propagation (1.13 ± 0.08 for cTnI-WT/dd, 0.96 ± 0.20 for cTnI-R145G/dd; Table 1) and thus might lead to an error of the second kind if the statistical decision of equal velocities for cTnI-WT/dd and cTnI-R145G/dd is accepted. Indeed, the sliding velocities of these reconstituted filaments measured at pCa 5 are significantly lower for cTnI-R145G/dd than for cTnI-WT/dd (0.92 ± 0.04 and 1.15 ± 0.07, $p < 0.05$). In this case, the results obtained with wild-type and R145G mutant cTnI would be congruent for the two types of measurements, actoS1-ATPase activity and thin filament sliding velocity. The basal normalized mean sliding velocities are similar for all four types of reconstituted thin filaments independent of R145G mutation or phosphorylation state of cTnI (Table 1, 24−40% of reference velocity, differences being statistically not significant). The number of moving filaments was much smaller at pCa 9.8 than at pCa values covering the rising phase of the activation curve (Figure 3A,B). The general course of these curves was not changed when more flow cell locations were inspected at pCa 9.8 in order to obtain approximately the same number of moving filaments as for lower pCa values (exemplified with cTnI-WT/pp in Figure 3A).

The Ca^{2+}-dependent activation of thin filament in vitro motility was in the same way affected by phosphorylation as the Ca^{2+}-dependent activation of actoS1-ATPase (Figure 3C,D). It is about 0.15 ± 0.08 pCa unit less sensitive ($p <$ 0.05) for cTnI-WT/pp compared to cTnI-WT/dd (Figure 3C). Bisphosphorylation of R145G mutant cTnI did not have a significant effect on the Ca^{2+} sensitivity of the in vitro filament sliding velocity (Figure 3D). However, this mutation of cTnI did not cause a significant shift of the Ca^{2+} activation curves of filament motility toward lower free Ca^{2+} concentrations as observed for the actoS1-ATPase activity with both states of cTnI phosphorylation. The cooperativity of these activation curves was not significantly changed by mutation R145G or bisphosphorylation of cTnI.

The results presented in Figure 3 report the movement capability of reconstituted thin filaments without reflecting the relative number of filaments at a location which are "switched on", i.e., that are moving at a given pCa with the observed average velocities. Figure 4 shows that activation of movement of the reconstituted thin filaments is not an on−off process but rather is a continuous function of the free Ca^{2+} concentration as has been reported previously for filaments controlled by the native bovine cardiac troponin complex (*35*). At pCa 9.8 about 3.8−8.3% of all filaments at observed locations are moving with the reported average velocities independent of filament type and phosphorylation state (Figure 4A,B). The moving fraction of filaments increases sigmoidally with the free Ca^{2+} concentration to a maximum of about 71.5−77.4% at pCa 5, again independent of filament type and phosphorylation state. Thus, about 25% of all reconstituted filaments could not be encouraged to move but about 88−95% of those evaluated with the in vitro

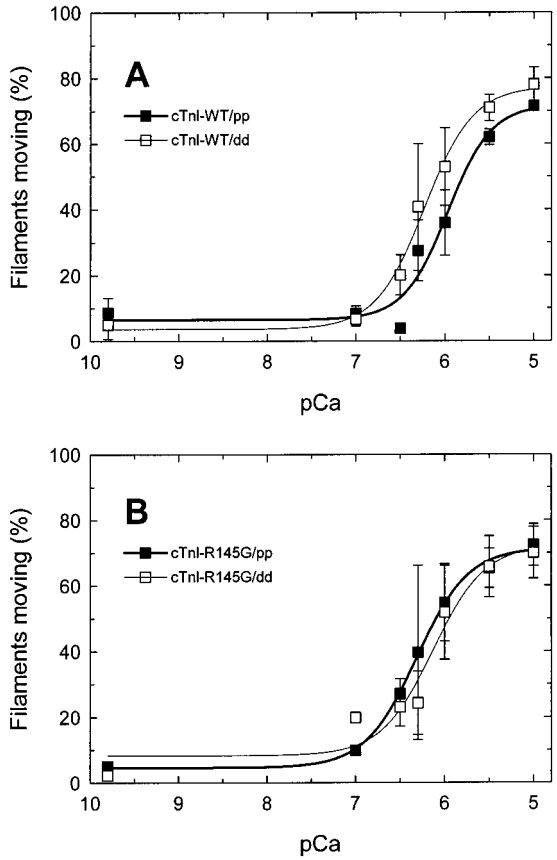

FIGURE 4: Fraction of moving filaments reconstituted with wild-type (A) or R145G mutant (B) cTnI in either the non- or the bisphosphorylated state as function of pCa. The number of filaments moving relative to the total number of filaments (260−1051) at each pCa was obtained from nine different sites randomly selected from three flow cells. The curves represent nonlinear least-squares fits to the data employing eq 1 (see Experimental Procedures). The values obtained for the fit parameters *a*, *b*, pCa_{50}, and *n* are 3.6 ± 3.5, 73.8 ± 5.9, 6.23 ± 0.06, 1.58 ± 0.36 (cTnI-WT/dd); 6.5 ± 5.5, 65.3 ± 11.3, 5.97 ± 0.14, 1.76 ± 0.81 (cTnI-WT/pp); 8.3 ± 6.6, 64.0 ± 12.4, 6.13 ± 0.16, 1.49 ± 0.75 (cTnI-R145G/dd); and 4.6 ± 1.7, 66.9 ± 2.6, 6.31 ± 0.03, 1.50 ± 0.16 (cTnI-R145G/pp).

motility assay were completely under control of the regulatory proteins and Ca^{2+}. This holds for wild-type and R145G mutated cTnI in both phosphorylation states. The average mean sliding velocity observed at pCa 9.8 with these four types of reconstituted thin filaments is less than 40% of the reference velocity (Figure 3A,B) but is due to less than 10% of all filaments (Figure 4A,B). Thus, the filaments contributing to this pool are in some way reconstituted and regulated but not completely blocked by the regulatory proteins. If a considerable fraction of those filaments were completely void of Tm and cTn, the measured average sliding velocity should be much closer to the reference level. The fractional number of filaments moving in the in vitro motility assay seems to reflect much better the inhibitory properties of the reconstituted filaments and thus the degree and quality of actin−Tm−cTn complex formation than the mean sliding velocity. The fraction of about 25% nonmovers in all reconstituted thin filament preparations investigated might rather be due to myosin than to the reconstituted thin filaments. Possible causes could be irreversibly inactivated myosin heads despite actin affinity purification prior to usage or unfavorable myosin surface density despite optimization of surface coating (see Experimental Procedures).

The differential effect of phosphorylation of each of the two adjacent serines in the cardiac specific extension of cTnI was further studied with the mutated forms cTnI-S22A and cTnI-S23A. The influence of phosphorylation of the remaining serine, Ser23 in cTnI-S22A and Ser22 in cTnI-S23A, on actoS1-ATPase activity and thin filament mean sliding velocity is shown in Figure 5. The maximum actoS1-ATPase activities obtained with nonphosphorylated cTnI-S22A (107% of reference level; Figure 5A and Table 1) and cTnI-S23A (71% of reference level; Figure 5B and Table 1) are not significantly different from those of the corresponding monophosphorylated cTnI-S22A and cTnI-S23A (89% and 60% of reference level, respectively; Figure 5A,B and Table 1). The same is true for the maximum normalized mean sliding velocity of these reconstituted thin filaments (cTnI-S22A/d 92%, cTnI-S22A/p 79%, cTnI-S23A/d 88%, and cTnI-S23A/p 75% of reference velocity, respectively; Figure 5C,D and Table 1).

There are, however, significant differences in the maximum actoS1-ATPase activity and the thin filament in vitro motility due to these mutants of cTnI when compared to nonphosphorylated wild-type cTnI. The maximum actoS1-ATPase activity obtained with phosphorylated cTnI-S22A is significantly lower ($p < 0.05$) than that with cTnI-WT/dd whereas that obtained with nonphosphorylated cTnI-S22A is not (compare Figures 2A and 5A; Table 1). In contrast, cTnI-S23A yields a significantly lower ($p < 0.02$) maximum actoS1-ATPase activity than that obtained with cTnI-WT/dd in both the non- and the monophosphorylated states (compare Figures 2A and 5B; Table 1). Thus, replacement of Ser23 by alanine seems already sufficient to cause the observed suppressing effects whereas replacement of Ser22 by alanine needs additional phosphorylation of Ser23 in order to produce the same degree of suppression. The same effect is observed if the sliding velocities of these filaments measured at pCa 5 are considered (compare Figures 3A and 5C,D), but it is not if the maximum velocities, *c*, estimated from the fit parameters, *a* and *b*, are compared (Table 1). On the basis of the measured sliding velocities, filaments reconstituted with cTnI-S22A/p (0.74 ± 0.05, $p < 0.005$), cTnI-S23A/d (0.87 ± 0.10, $p < 0.05$), and S23A/p (0.74 ± 0.13, $p < 0.05$) move significantly slower at pCa 5 than those with cTnI-WT/dd (1.15 ± 0.07). These results suggest that phosphorylation of serine 23 alone may already be sufficient for causing the suppressing effects on the maximum actoS1-ATPase activity and the maximum thin filament in vitro sliding velocity seen upon phosphorylation of both regulatory important serines of cTnI. There was no convincing evidence for a change in Ca^{2+} sensitivity of these thin filament-linked properties measured due to one of these serine mutated cTnI forms, neither in the non- nor in the monophosphorylated state. The cooperativity of these processes was not significantly altered by these mutations either.

DISCUSSION

The functional properties of the thin filaments reconstituted with either wild-type or mutant cTnI in the nonphosphorylated or the fully phosphorylated state (i.e., monophosphorylated for cTnI-S22A and cTnI-S23A or bisphosphorylated for cTnI-WT and cTnI-R145G) are well controlled by Ca^{2+}. The actoS1-ATPase activity and the in vitro motility measured with these filaments are significantly influenced

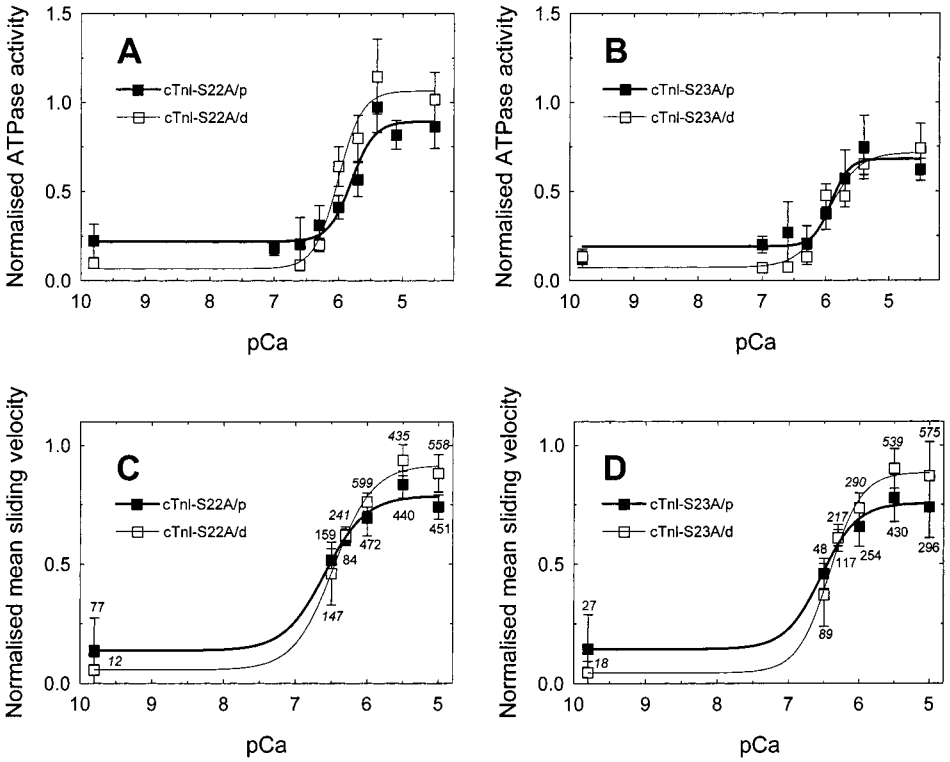

FIGURE 5: Ca^{2+}-dependent actoS1-ATPase activity (A, B) and mean sliding velocity (C, D) of thin filaments containing S22A (A, C) or S23A (B, D) mutant cTnI in either the non- or the monophosphorylated state. Thin filament-activated myosin S1-ATPase activity and mean sliding velocity are given as mean values ± SEM. The data were normalized to the F-actin-activated myosin S1-ATPase activity and the mean sliding velocity of phalloidin−TRITC-stabilized F-actin, respectively, measured under the corresponding conditions. The number of filament paths of a velocity data set is given by the number close to the corresponding error bar (italic for nonphosphorylated cTnI). The curves represent nonlinear least-squares fits to the data employing eq 1 (see Experimental Procedures). The values of the fit parameters *a*, *b*, pCa_{50}, and *n* are compiled in Table 1.

by some of these mutations and/or phosphorylations of cTnI. In the presence of wild-type cTnI, the actoS1-ATPase activity is significantly more Ca^{2+} sensitive for the nonphosphorylated than for the bisphosphorylated cTnI. Phosphorylation of the two adjacent serines, 22 and 23, of wild-type cTnI is shifting the activation curve by about 0.21 ± 0.06 ($p < 0.005$) pCa unit toward higher free Ca^{2+} concentrations without changing the cooperativity of the activation process (Figure 2C). A similar rightward shift of the activation curve ($\Delta pCa_{50} \sim 0.15 \pm 0.08$, $p < 0.05$) has been found for the in vitro sliding velocity of filaments containing bisphosphorylated compared to nonphosphorylated wild-type cTnI (Figure 3C). These effects can be explained by a decreased rate of myosin S1 binding to the regulated actin filaments which was observed by some of us with the same types of filaments under pseudo-first-order conditions due to bisphosphorylation of cTnI (*12*). It might ultimately be caused by a increased rate of Ca^{2+} dissociation from cTnC which has been seen in the presence of bisphosphorylated cTnI (*11*). At a given pCa this will tend to stabilize the blocked state of the actin−Tm−cTn conformation (*37*).

These observations are in agreement with studies on skinned cardiac muscle preparations of porcine heart which report a similar decrease in the Ca^{2+} sensitivity of force development upon phosphorylation of the corresponding serines by PKA (*14*). The C-terminal one of the two adjacent serines is phosphorylated more rapidly in human (*38*) and mouse cTnI (*13*), but the bisphosphorylated state seems to confer the characteristic reduction in Ca^{2+} sensitivity to the actomyosin system (*12*, *13*, *23*). Skinned fiber and reconstituted filament studies employing cTnI-S22A and cTnI-S23A did not find evidence for an effect on the Ca^{2+} sensitivity when only Ser22 or Ser23 was phosphorylated (*13*, *23*). This is confirmed by the present study using the same mutant proteins, cTnI-S22A and cTnI-S23A. However, we have found suppressing effects of one of these mutations, S23A, as well as of phosphorylated cTnI-S22A on both the maximum actoS1-ATPase activity (compare Figures 2A and 5A,B) and the maximum average sliding velocity of reconstituted thin filaments (compare Figures 3A and 5C,D). A functional effect due to phosphorylation of only one of the two serines has been proposed tentatively because mono- and bisphosphorylation had caused different conformational changes within cTnI (*23*). The present results suggest that the observed suppressing effects may mainly be due to serine 23 because replacement by alanine or phosphorylation of this residue was already leading to significantly reduced maximum response levels compared to cTnI-WT/dd. A comparable decrease in the maximum actoS1-ATPase activity and the maximum filament sliding velocity was observed when both serine residues of wild-type cTnI were phosphorylated (Figures 2A and 3A). These suppressing effects are new findings which inevitably had to be missed in comparable studies on the effect of cTnI phosphorylation on the contraction of skinned cardiac muscle (*13*). There, normalization of a measured force to the maximum force was necessary in order to compensate for varying degrees of cTnC−cTnI reconstitution and to enable comparison of the data as a function of the phosphorylation state of cTnI. A study on single skinned rat cardiac myocytes did not find

an effect on maximum tension generation upon PKA treatment (*9*). It does, however, not provide information about the degree of cTnI phosphorylation nor can it differentiate between effects due to cTnI and/or myosin binding C-protein phosphorylation. The latter was also occurring and is known to increase the maximum Ca^{2+}-activated force (*10*).

In the virtual absence of Ca^{2+}, filaments reconstituted with both cTnI-WT/dd and cTnI-WT/pp are leading to an inhibition of actoS1-ATPase and filament in vitro motility to comparable levels (Figures 2A and 3A). Thus, phosphorylation or dephosphorylation of Ser22 and/or Ser23 of cTnI does not seem to influence the inhibitory properties of the regulatory system at low free Ca^{2+} concentrations. This is in strong contrast to the marked effect that the phosphorylation of both serines has on the regulatory system in the maximum Ca^{2+}-activated state. The fact that no complete inhibition was reached at pCa 9.8 indicates that a fraction of the reconstituted thin filaments is not entirely or not correctly assembled with the regulatory proteins. This amounts to about 5−12% of all Ca^{2+}-responsive filaments as has been estimated from the fractional number of filaments moving in the in vitro motility assay (Figure 4). Non-Ca^{2+}-responsive filaments will contribute neither to the measured actoS1-ATPase activity nor the in vitro filament sliding velocity.

In a second approach we have investigated the regulatory properties of R145G-mutated cTnI which is correlated with the development of fHCM in humans (*17*, *18*). The functional properties of thin filaments containing this mutated cTnI were in two major aspects different from those containing wild-type cTnI. First, the mutation R145G mimics the effect of bisphosphorylation of wild-type cTnI on both the maximum actoS1-ATPase activity (Figure 2A, B) and the maximum average filament sliding velocity (Figure 3A,B). It renders the actomyosin system at maximum Ca^{2+} activation insensitive to phosphorylation; i.e., neither the maximum actoS1-ATPase activity nor the maximum average sliding velocity is significantly higher in the presence of cTnI-R145G/dd compared to cTnI-R145G/pp (Figures 2B and 3B). A reduced maximum ATPase activity has been reported recently also for myofibrils of porcine cardiac muscle reconstituted with human cTnI-R145G in comparison with human wild-type cTnI (*39*); the phosphorylation state of cTnI in the reconstituted myofibrils was, however, not looked at. This study (*39*) and one with reconstituted thin filaments containing recombinant human wild-type or R145G mutant cTnI (*18*) report a reduced inhibition of the thin filament-activated myosin ATPase activity for the mutant cTnI under relaxing conditions. We have not observed a significant effect at relaxing free Ca^{2+} concentrations due to this mutation or phosphorylation/dephosphorylation of cTnI-R145G neither on the actoS1-ATPase activity nor on the in vitro filament motility (Figures 2B and 3B). This might be partially due to different experimental conditions [myofibrils (*39*), 37 °C (*18*), unknown cTnI phosphorylation state (*18*, *39*)] and reconstitution procedures which are known to affect the behavior of the complex thin filament structure (*12*).

The second major effect found in the present study due to the mutation R145G of cTnI was a significantly increased Ca^{2+} sensitivity in the activation of actoS1-ATPase. This is reflected by a midpoint shift of the activation curves obtained in the presence of non- and bisphosphorylated cTnI-R145G of about 0.58 ± 0.07 ($p < 0.0001$) and 0.63 ± 0.12 ($p < 0.0001$) pCa unit, respectively, toward lower free Ca^{2+} concentrations in comparison with wild-type cTnI in the corresponding phosphorylation state (Figure 2C,D). This finding is in agreement with studies on the myosin ATPase activity of myofibrils (*39*) and reconstituted thin filaments (*18*) which report similarly enhanced Ca^{2+} sensitivities of about 0.29 and 0.56 pCa unit, respectively, for regulatory systems containing cTnI-R145G. These studies do, however, not provide information about the phosphorylation state of the cTnI in focus. A corresponding effect due to this mutation was not apparent in the in vitro motility of the same reconstituted filaments. This discrimination between ATPase activity and in vitro motility appears dubious because of the direct coupling between the enzymatic and the mechanical events during the cycling interaction of myosin with the actin filament.

The structural change in the regulatory system of thin filaments caused by phosphorylation of Ser22 and Ser23 of cTnI seems to be linked with the structural alteration caused by the mutation R145G in cTnI. The mutation mimics and makes permanent the suppressing effects of cTnI bisphosphorylation on maximum actoS1-ATPase activity and in vitro filament motility but inverses the rather desensitizing effects of cTnI bisphosphorylation on both of these Ca^{2+}-dependent processes.

ACKNOWLEDGMENT

We thank Albrecht Wegner for providing the skeletal muscle actin, Friedrich W. Herberg for providing the catalytic subunit of PKA, and Nick Carter, MCRI, Oxted, for making the tracking software RETRAC available as freeware. We also thank Ludwig M. G. Heilmeyer, Jr., for helpful suggestions and discussions.

REFERENCES

1. Mittmann, K., Jaquet, K., and Heilmeyer, L. M. G., Jr. (1990) *FEBS Lett. 273*, 41−45.
2. Tobacman, L. S. (1996) *Annu. Rev. Physiol. 58*, 447−481.
3. Solaro, R. J., and Rarick, H. M. (1998) *Circ. Res. 83*, 471−480.
4. Gordon, A. M., Homsher, E., and Regnier, M. (2000) *Physiol. Rev. 80*, 853−923.
5. England, P. J. (1975) *FEBS Lett. 50*, 57−60.
6. Venema, R. C., and Kuo, J. F. (1993) *J. Biol. Chem. 268*, 2705−2711.
7. Gruen, M., Prinz, H., and Gautel, M. (1999) *FEBS Lett. 453*, 254−259.
8. Li, L., Desantiago, J., Chu, G., Kranias, E. G., and Bers, D. M. (2000) *Am. J. Physiol. Heart Circ. Physiol. 278*, H769−H779.
9. Hofmann, P. A., and Lange, J. H. (1994) *Circ. Res. 74*, 718−726.
10. Kunst, G., Kress, K. R., Gruen, M., Uttenweiler, D., Gautel, M., and Fink, R. A. H. (2000) *Circ. Res. 86*, 51−58.
11. Robertson, S. P., Johnson, J. D., Holroyde, M. J., Kranias, E. G., Potter, J. D., and Solaro, R. J. (1982) *J. Biol. Chem. 257*, 260−263.
12. Reiffert, S. U., Jaquet, K., Heilmeyer, L. M. G., Jr., Ritchie, M. D., and Geeves, M. A. (1996) *FEBS Lett. 384*, 43−47.
13. Zhang, R., Zhao, J., and Potter, J. D., (1995) *J. Biol. Chem. 270*, 30773−30780.
14. Zhang, R., Zhao, J., Mandveno, A., and Potter, J. D. (1995) *Circ. Res. 76*, 1028−1035.
15. Wolff, M. R., Buck, S. H., Stoker, S. W., Greaser, M. L., and Mentzer, R. M. (1996) *J. Clin. Invest. 98*, 167−176.

16. Bodor, G. S., Oakeley, A. E., Allen, P. D., Crimmins, D. L., Ladenson, J. H., and Anderson, A. A. W. (1997) *Circulation 96*, 1495−1500.
17. Kimuara, A., Harada, H., Park, J. E., Nishi, H., Satoh, M., Takahashi, M., Hiro, S., Sasaoka, T., Ohbuchi, N., Nakamura, T., Hwang, T. H., Choo, J. A., Chug, K., S., Hasegawa, A., Nagai., R., Okazaki, O., Nakamura, H., Matsuzaki, M., Sakamoto, T., Toshima, H., Koga, Y., Imaizumi, T., and Sasazuki, T. (1997) *Nat. Genet. 16*, 379−382.
18. Elliott, K., Watkins, H., and Redwood, C. S. (2000) *J. Biol. Chem. 275*, 22069−22074.
19. Mesnard, L., Samson, F., Espinasse, I., Durand, J., Neveux, J. Y., and Mercadier, J. J. (1993) *FEBS Lett. 328*, 139−144.
20. Schenk, P. M., Baumann, S., Mattes, R., and Steinbiss, H. H. (1995) *BioTechniques 19*, 196−198.
21. Reiffert, S. U., Jaquet, K., Heilmeyer, L. M. G., Jr., and Herberg, F. W. (1998) *Biochemistry 39*, 13516−13525.
22. Babu, A., Su, H., Ryu, Y., and Gulati, J. (1992) *J. Biol. Chem. 267*, 15469−15474.
23. Reiffert, S., Maytum, R., Geeves, M., Lohmann, K., Greis, T., Blüggel, M., Meyer, H. E., Heilmeyer, L. M. G., Jr., and Jaquet, K. (1999) *Eur. J. Biochem. 261*, 40−47.
24. Bradford, M. M. (1976) *Anal. Biochem. 72*, 248−254.
25. Laemmli, U. K. (1970) *Nature 227*, 680−685.
26. Swiderek, K., Jaquet, K., and Heilmeyer, L. M. G., Jr. (1988) *Eur. J. Biochem. 176*, 335−342.
27. Teubner, A., and Wegner, A. (1998) *Biochemistry 37*, 7532−7538.
28. Smillie, L. B. (1982) *Methods Enzymol. 85*, 234−241.
29. Margossian, S. S., and Lowey, S. (1982) *Methods Enzymol. 85*, 55−71.
30. Webb, E. (1992) *Proc. Natl. Acad. Sci. U.S.A. 89*, 4884−4887.
31. Moisescu, D. G., and Thieleczek, R. (1978) *J. Physiol. 275*, 241−262.
32. Fabiato, A. (1979) *J. Physiol. 75*, 463−505.
33. Kron, S. J., Toyoshima, Y. Y., Uyeda, T. Q. P., and Spudich, J. A. (1991) *Methods Enzymol. 196*, 399−416.
34. RETRAC, tracking software by Nick Carter, Marie Curie Research Institute, The Chart, Oxted, Surrey RH8 0TL, U.K.
35. Homsher, E., Kim, B., Bobkova, A., and Tobacman, L. S. (1996) *Biophys. J. 70*, 1881−1892.
36. Melki, R., Fievez, S., and Carlier, M.-F. (1996) *Biochemistry 35*, 12038−12045.
37. McKillop, D. F. A., and Geeves, M. A. (1991) *Biochem. J. 279*, 711−718.
38. Jaquet, K., Thieleczek, R., and Heilmeyer, L. M. G., Jr. (1995) *Eur. J. Biochem. 231*, 486-490.
39. Takahashi-Yanaga, F., Morimoto, S., and Ohtsuki, I. (2000) *J. Biochem. 127*, 355−357.

BI0115232